ICAS-98-3,8,3

A98-31562

AERODYNAMIC CHARACTERISTICS OF UNCONVENTIONAL AIRCRAFT CONFIGURATIONS

Z. Pátek
VZLU, Aeronautical Research and Test Institute
Prague, Czech Republic

L. Smrcek
Department of Aerospace Engineering
University of Glasgow, Scotland, UK

Abstract

This paper describes the wind-tunnel testing of some unconventional aircraft configurations of specially designed wind tunnel models in the 1.8m low-speed wind tunnel at VZLU, Aeronautical Research and Test Institute in Prague, and numerical validation of CFD package RAMPANT performed in the computerised fluid dynamic laboratory at the Department of Aerospace Engineering, The University of Glasgow. The numerical validation is being conducted by the University of Glasgow as a part of the ongoing research collaboration between both institutions. The wind-tunnel test programme had two aims

- to provide basic aerodynamic data on the effects of unconventional aircraft configurations with a view to assessing the degree to which specific design features such as a combination of canard, wing and tail-plane are beneficial to aircraft aerodynamic performance
- to provide an aerodynamic database for numerical validation

The aerodynamic data for different geometrical aircraft configurations with the same wing, fuselage, tail and canard surfaces were compared. The results show that the magnitude of lift, drag and pitching moment depends on the angle of attack and various positions of canard, wing and tail with respect to one another.

Nomenclature

C_l	=	lift coefficient	
α	=	angle of attack	
C_D	=	drag coefficient	
C_{mo}	=	zero lift pitching moment coefficent (positive nose up)	
C_m	=	pitching moment coefficient (positive nose up)	
c	=	wing chord	
h_{wt}	=	tail horizontal position	(see Fig. 1)
v_{wt}	=	tail vertical position	(see Fig. 1)
h_{wc}	=	canard horizontal position	(see Fig. 1)
v_{wc}	=	canard vertical position	(see Fig. 1)

Introduction

Aircraft development in many ways means to improve it's aerodynamic characteristics all the time. This aim can be achieved by modifying existing classical aircraft configurations or by adopting the more radical approach of unconventional aircraft geometrical configurations. The most common way of dealing with such a problem is to delete the longitudinal stabiliser aft of the wing and substitute it by something else. Such an aircraft configuration is being used in both civilian and military applications. The purpose of this research was to find the configuration using canard, wing or tail which will improve aircraft performance in comparison to the conventional aircraft surface arrangement.

Unconventional aircraft geometry has been known since the beginning of aviation, but it was only during the sixties that some of these aircraft got past the prototype stage into serial production. The first of these were military aircraft and in the late seventies the first civil canard application was used for sport/recreation aircraft design. In 1985 the prototype of a new canard commuter aircraft was built with the view of bringing the project into serial production. The trial was successful, however, serial production was later suspended due to the high cost and technical problems of the aircraft involved. The results of analytical analysys of some unconventional aircraft configurations were published mainly by Keith[1], Rokhsaz and Selberg[2], [3], [4].
Some experimental work by Feistel[5], Ostowari[6] had been studied prior to the research to identify the wind tunnel set-up and model geometry.

The research which has been undertaken and is also presented in this paper examines the geometric parameters of the aircraft model and the effect on the aerodynamic characteristics such as, lift curve gradient and maximum lift coefficient, minimum drag coefficient and pitching moment coefficient. The experimental tests results for all selected model variants are presented in this paper. These data create an aerodynamic database for numerical modelling verification.

Wind Tunnel Model

A specially designed modular aircraft wind tunnel model was made which allowed changes to aircraft configuration. The metal aircraft model was constructed from modules such as canard, fuselage, wing and tail. The basic model dimensions are shown in Fig. 1. Modular construction was used to enable the creation of three basic aircraft configurations such as conventional wing-tail aircraft configuration, unconventional with foreplane canard-wing and canard-wing-tail aircraft configurations. It was also possible to change the relative position of canard, wing and tail as shown in Fig. 1.

The wing was rectangular with a profile NACA 0015 along the span, without dihedral or twist. The modular aircraft model allowed use of wing in low or high configuration. Canard and horizontal stabilisers were also of rectangular shape with an area 30% of the wing, NACA 0012 profile and without dihedral or twist. It was possible to place the canard in nine positions on the forward fuselage or to take it away. Also, the horizontal tail could be fixed in four positions on the fin or taken away.

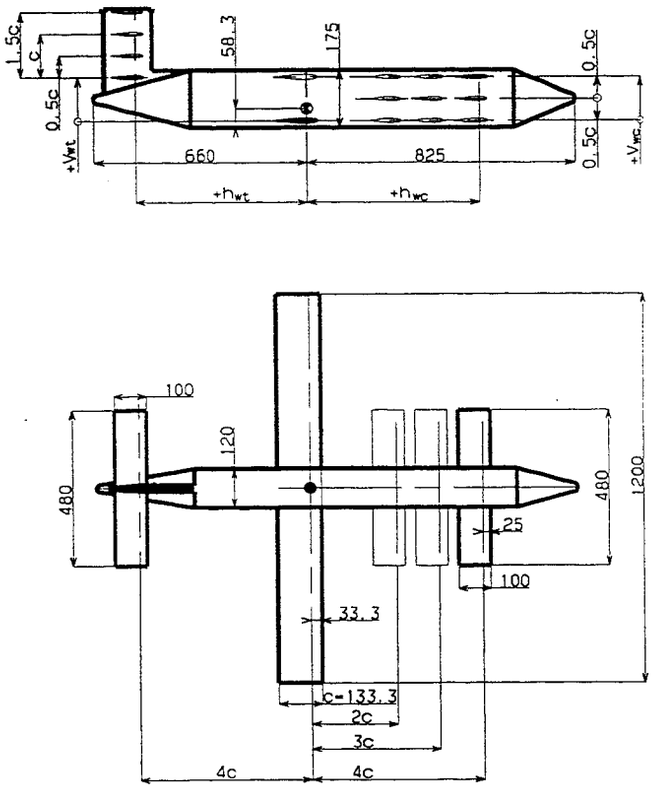

FIGURE 1 - Wind Tunnel Model
[dimensions in mm]

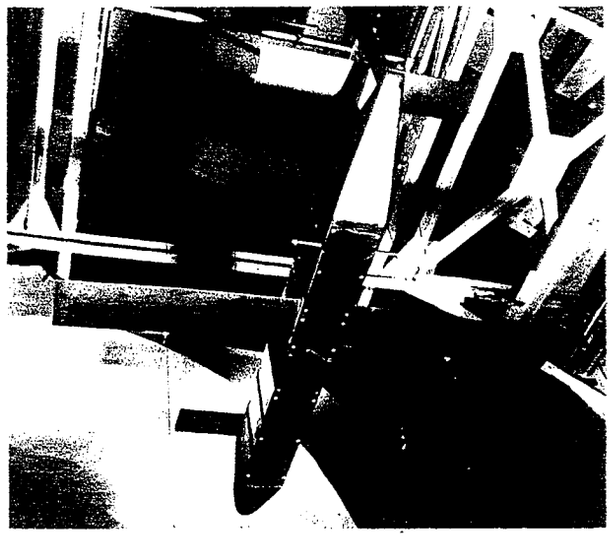

FIGURE 2 - Model in the Wind Tunnel

Wind Tunnel Test Set-up

All tests were conducted in the 1.8 m low speed wind tunnel at VZLU, Aeronautical Research and Test Institute in Prague in the Czech Republic[7]. This institute has provided very good quality wind tunnel facilities for the Czech aircraft industry for many years. The particular wind tunnel used in this study was an atmospheric open-section, closed return, with a maximum velocity of 55 m/s. Forces and moments were measured on a six component overhead gravitational balance. The model was mounted in the wind tunnel by a system of connecting wires. The model hanging in the wind tunnel can be seen in Fig. 2. The Reynolds Number based on the wing chord was 3.35×10^5.

For calculations of non dimensional force coefficients reference used was the wing area including part of the wing shadowed by the fuselage.

The basic characteristic length for pitching moment coefficient calculation was the wing mean aerodynamic chord.

The reference point for quarter chord pitching moment coefficient calculation, for all aircraft configurations measured, was the centre of gravity positioned as shown in Fig. 1.

All measurements were without sideslip.

Experimental Data Analysis

The main features of the results from the wind-tunnel test programme are presented and analysed in this section.

Selected aerodynamic data are represented by lift, drag and pitching moment coefficients and are shown and analysed for three basic aircraft configurations.

1 Conventional aircraft wing-tail configuration (for reference only)
2 Canard-wing configuration.
3 Canard-wing-tail configuration.

The various combination of vertical and longitudinal position with respect to one another of canard, wing and tail is listed in the tables for each aircraft configuration measured.

Wing-Tail Configuration

Measured in the wind-tunnel were six combinations of wing and tail relative positions. Three combinations were for low wing configuration and three for high wing configuration. The combinations and geometry of wing and tail that were tested are listed in Table 1. For high wing configuration the vertical position of the tail was in the region $c \le v_{wt} \le 2c$. Horizontal position of the tail was kept constant at $h_{wt} = 4c$. The tail incidence with respect to the wing was zero.

Figures 3, 4 and 5 present experimental data for a wing-tail configuration.

Configuration Wing-Tail	h_{wt}	v_{wt}
High Wing	4c	0
		0.5c
		1.5c
Low Wing	4c	1c
		1.5c
		2c

TABLE 1

Lift Curve Slope, C_{L_α}

Fig. 3 presents the measured lift curve slope for each of the six configurations examined in the study. From the figure it is possible to observe that both the slope and magnitude of lift coefficient are affected by the vertical position of the tail relative to the high or low wing configuration. Maximum recorded increase in C_{L_α} derivative was in the region of 0.15 rad^{-1}. This was due to the reduction of wing and fuselage effect on the tail flow (downwash).

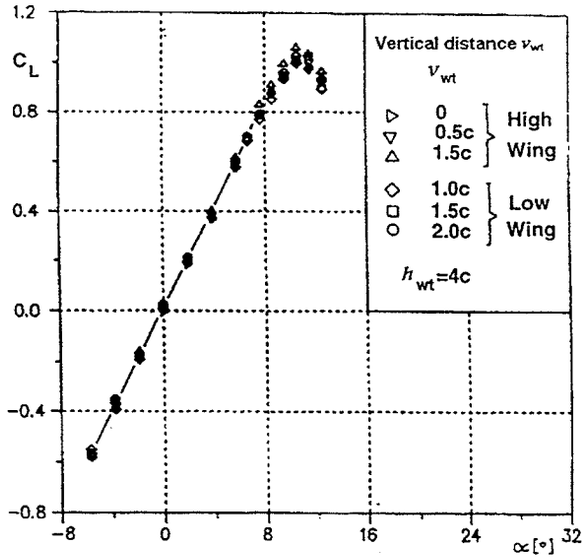

FIGURE 3 - Conventional Configuration, Tail Effect

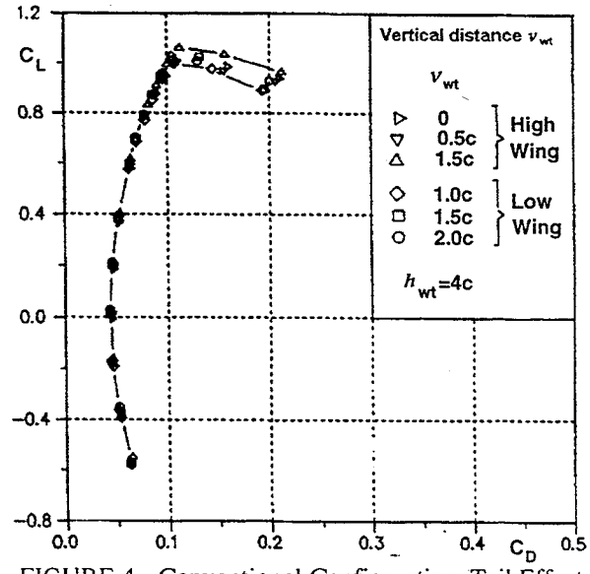

FIGURE 4 - Conventional Configuration, Tail Effect

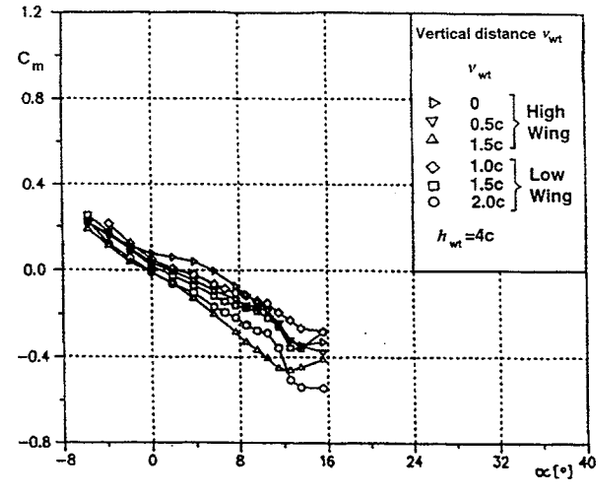

FIGURE 5 - Conventional Configuration, Tail Effect

Maximum Lift Coefficient, $C_{L\,max}$

Increase in vertical distance, v_{wt}, between the wing and tail for both low and high wing configuration was the main reason for increment in $C_{L\,max}$ as shown in Fig 3. This effect is again explained by the reduction of wing and fuselage effect on the tail flow.

Minimum Drag Coefficient, $C_{D_{min}}$

The experimental results are illustrated in Fig. 4. In the case of high wing configuration minimum drag coefficient was decreasing with increased vertical distance, v_{wt}. But for higher values of v_{wt} decrease in $C_{D_{min}}$ was not so significant. Maximum $C_{D_{min}}$ reduction occurred when the distance v_{wt} was between zero and 1.5c and was $\Delta C_{D\,min}$ = 0.0012.
In the case of low wing aircraft configuration minimum drag coefficient was not affected with change in vertical position of tail on the fin.

Pitching Moment Coefficient, C_m

Fig. 5 shows wind tunnel experimental pitching moment coefficient curves. From this figure it can be observed that increased vertical distance between the wing and tail make the curve slope more negative, thus the neutral point was shifting backwards. Also, by increasing the distance between the wing and tail the downwash on the tail was reduced and this resulted in a decrease in zero lift pitching moment, C_{mo}.

Canard-Wing Configuration

The results from the experiments which were carried out to find the effect of various canard-wing positions, with respect to one another, on aerodynamic forces and pitching moment are presented in Figures 6, 7, 8, 9, 10 and 11. Table 2 shows that eighteen combinations canard-wing which were measured in the wind tunnel. Nine variations of measurement were a combination of canard and high wing configurations. In this case horizontal distance between canard and the wing varied in the region $2c \le h_{wc} \le 4c$ and the vertical distance in the region of, $-c \le v_{wc} \le 0$. The remaining nine configurations were canard and the low wing. The horizontal distance between canard and wing changed in the region $2c \le h_{wc} \le 4c$ and the vertical distance in the region of $0 \le v_{wc} \le c$.

Lift Curve Scope, C_{L_a}

As shown in Figures 6 and 9 the variation of lift force with angle of attack was to be almost linear in the - 6 < α < 7 degree range. A slight increase in lift curve slope due to the increased h_{wc} distance is noticable in the linear range of C_{L_a} for both low and high wing configuration. Changes in vertical distance, v_{wc}, did not influence the lift curve slope.

Configuration Canard-Wing	h_{wt}	v_{wc}
High Wing	2c	-1c
		-0.5c
		0
	3c	-1c
		-0.5c
		0
	4c	-1c
		-0.5c
		0
Low Wing	2c	0
		0.5c
		1c
	3c	0
		0.5c
		1c
	4c	0
		0.5c
		1c

TABLE 2

Maximum Lift Coefficent, $C_{L\,max}$

As it can be seen in Figures 6, 7, 9, and 10 the horizontal distance between canard and wing, h_{wc}, has not affected the maximum lift coefficients but the canard vertical position with respect to the wing affected $C_{L\,max}$ noticeably. The lowest $C_{L\,max}$ was recorded for high wing configuration when the vertical distance between canard and wing was v_{wc} = -0.5c. In this configuration the canard unfavourably affected the flow over the wing, particularly in the region of angle of attack corresponding to $C_{L\,max}$.

Minimum Drag Coefficient, $C_{D\,min}$

Shortening of the horizontal distance between canard and wing influenced the minimum drag coefficient only in the region of h_{wc} between 3c and 2c when the reduction of $C_{D\,min}$ was only 0.001 as can be Figures 7 and 10.

Increased vertical distance between the canard and the wing contributed to the reduction of minimum drag coefficient in both cases when the canard was shifted above or below the wing level. The highest C_{Do} was recorded when v_{wc} = 0.

Pitching Moment Coefficient, C_m

As indicated in Figures 8 and 11 pitching moment curve was affected by the horizontal distance, h_{wc}, between the canard and the wing in the case of high and low wing configurations. For increased h_{wc} the neutral point moved forward resulting in a reduction of longitudinal static stability.

Change in vertical distance between canard and wing v_{wc} was followed by a slight change in zero lift pitching moment coefficient. This was due to the fact that the change in vertical canard position with respect to the centre of gravity also changed canard drag moment which contribute to the overall pitching moment. The distance, v_{wc}, did not affect the curve gradient.

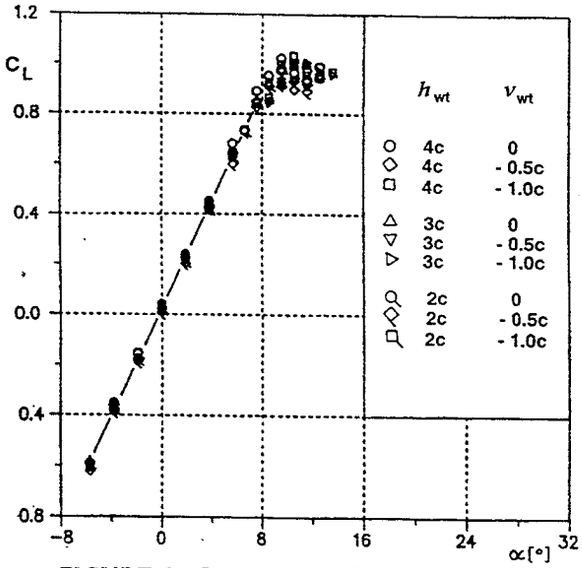

FIGURE 6 - Canard Wing Configuration with High Wing, Canard Effect.

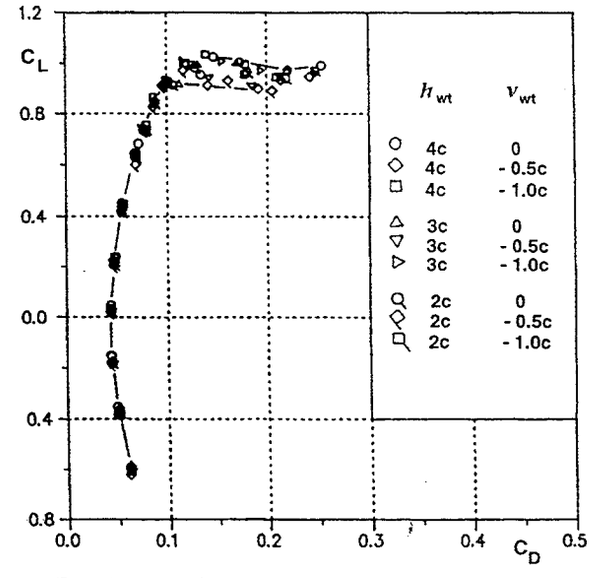

FIGURE 7 - Canard Wing Configuration with High Wing, Canard Effect.

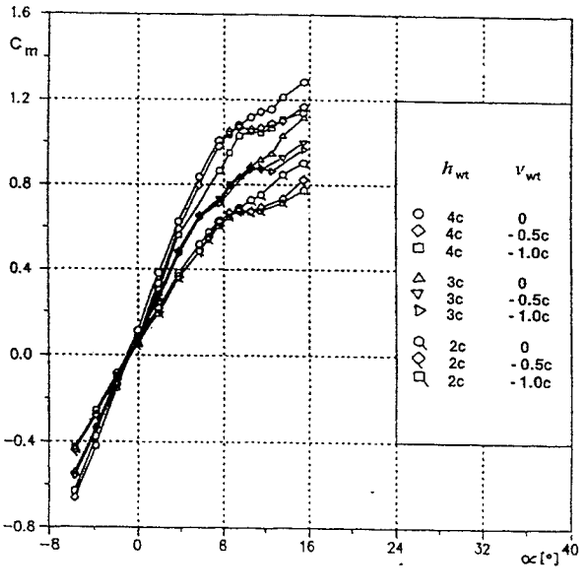

FIGURE 8 - Canard Wing Configuration with

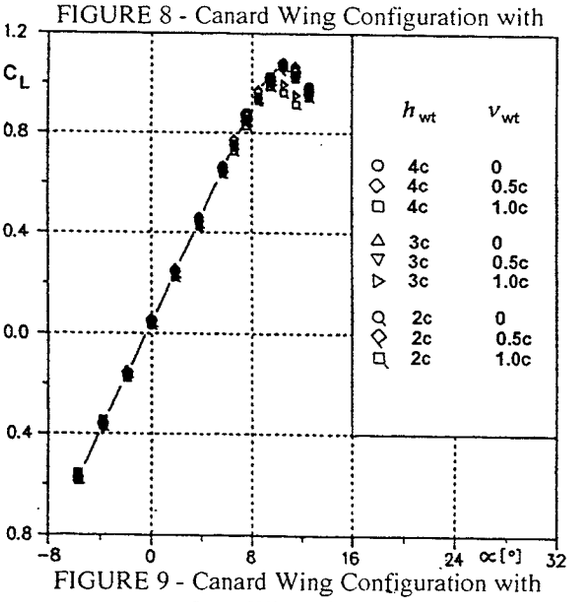

FIGURE 9 - Canard Wing Configuration with Low Wing, Canard Effect

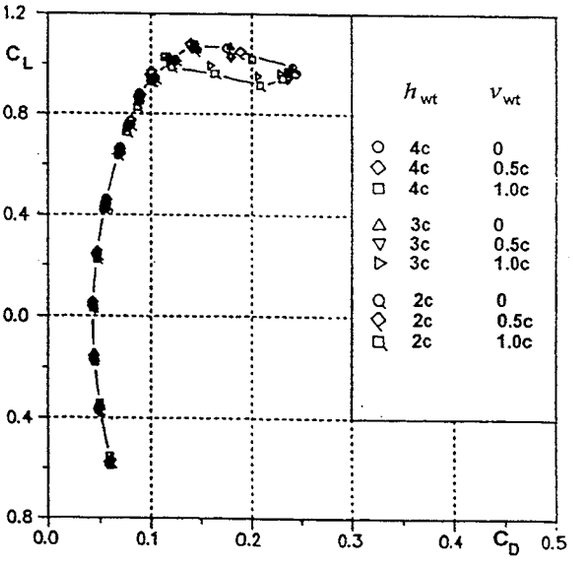

FIGURE 10 - Canard Wing Configuration with Low Wing, Canard Effect.

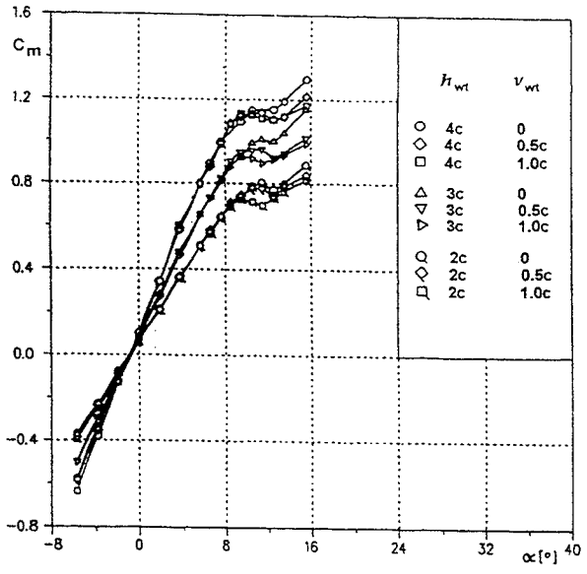

FIGURE 11 - Canard Wing Configuration with Low Wing, Canard Effect.

Canard-Wing-Tail Configuration

The experimental programme involved tests of twenty two different canard-wing-tail aircraft configurations with relative positions to each other as stated in Table 3.

Configuration Canard-Wing-Tail	h_{wc}	v_{wc}	h_{wt}	v_{wt}
High Wing	2c	-1c	4c	1.5c
		-0.5c		
		0		
	3c	-1c		
		-0.5c		
		0		
	4c	-1c		
		-0.5c		
		0		
	4c	-0.5c	4c	0
		-0.5c		0.5c
Low Wing	2c	0	4c	1.5c
		0.5c		
		1c		
	3c	0		
		0.5c		
		1c		
	4c	0		
		0.5c		
		1c		
	4c	1c	4c	1c
		1c		2c

TABLE 3

Half of the model configurations were with high wing. In nine cases the canard position was adjusted so that the horizonal and vertical distance from the wing were in the region $2c \le h_{wc} \le 4c$, $-c \le v_{wc} \le 0$ while the tail was in the fixed position $h_{wt} = 2c$ and $v_{wt} = 1.5c$. In two cases when canard position was at $h_{wc} = 4c$ and $v_{wc} = -0.5c$ the tail position was changed to $h_{wt} = 4c$ and $v_{wt} = 0$ and $v_{wt} = 0.5$ and the effect on the aerodynamic characteristics observed.

The other half of the model configurations were with low wing. Also in nine cases the canard position was adjusted so that the horizontal and vertical distances from the wing were in the region $2c \le h_{wc} \le 4c$, $0 \le v_{wc} \le 1c$ while the tail was in the fixed position $h_{wt} = 4c$ and $v_{wt} = 1.5c$. In two cases the canard was placed at $h_{wc} = 4c$ and $v_{wc} = 1c$ the tail position was adjusted to $h_{wt} = 4c$, $v_{wt} = 1c$ and $v_{wt} = 2c$ and the effect on the aerodynamic characteristics observed.

The results are presented in Figures 12 - 20.

Lift Curve Slope, C_{L_α}

If the horizontal canard distance from the wing h_{wc} is increased from 2c to 4c, according to Figures 12, 15 and 18, the increase in the lift curve gradients is about 0.1 rad^{-1} in the linear range of C_L.

The vertical distance between canard and wing influenced the lift curve slope by 0.4 rad in some model configurations. This effect was not observed in the canard-wing configuration nor did the vertical position of tail affect C_{L_α} in the case of the conventional wing-tail configuration. This could lead to the explanation that the canard affected the flow over the tail directly and also at the same time affected the wing flow and then downwash which resulted in different tail flow characteristics compared with conventional wing-tail configurations.

When the vertical distance between the tail and canard $(v_{wt} - v_{wc})$ was less than 1.5c, the tail was affected the most by the canard and this resulted in the reduction of C_{L_α}.

The effect of the vertical distance between the wing and the tail on C_{L_α} can be expected to be the same as in the case of conventional model configuration. This means increased vertical distance, v_{wt}, will result in a slight increase in C_{L_α}.

Maximum Lift Coefficient, $C_{L_{max}}$

In high wing configuration the horizontal distance between canard and wing, h_{wc}, did not affect $C_{L_{max}}$, but in the case of low wing configuration increase in h_{wc} resulted in a slight positive increment in $C_{L_{max}}$.

As Figures 12, 13, 15 and 16 show, for the canard-wing-tail confirguration, the vertical distance between canard and wing, v_{wc}, affected $C_{L_{max}}$ in the same way as in the case of canard-wing configuration. In the case of v_{wc} = - 0.5c and the critical angle of attack, decrease in $C_{L_{max}}$ was recorded. This was due to the unfavourable canard effect on the wing flow.

From the similarity between results observed for canard-wing and canard-wing-tail configurations it is possible to conclude that relative position of canard and tail does not affect $C_{L_{max}}$ significantly.

Minimum Drag Coefficient, $C_{D_{min}}$

According to the experimental results presented in Figures 13, 16 and 19 changes in position of both canard and tail surface did not affect minimum drag coefficient.

Pitching Moment Coefficient, C_m

Pitching moment curves as seen in Figures 14 and 17 were significantly affected by two geometrical parameters of the model. Firstly, it was the horizontal distance between the canard and the wing, h_{wc}, when increased then the neutral point is shifts forward and pitching moment curve slope is increased.

Secondly, the geometrical parameter which affected pitching moment was the canard vertical position, v_{wc}, and the tail vertical position, v_{wt}. This could be explained by analysing and comparing experimental results for different model geometrical configurations. Even this effect was not observed in the case of canard-wing and conventional wing-tail configurations it was possible to conclude that, for example, the differences in the pitching moment curves, between conventional and canard-wing-tail configurations, were the result of the canard flow effect on the tail. This was done directly by canard flow wake and also by canard effect on the wing flow and it's downwash which also affect and change tail flow characteristics.

The experiments show that a significant change in pitching moment coefficient which occurs in the practical range of angle of attack are related to the direct effect of the canard on the tail. This effect was significantly reduced by increasing the vertical distance, v_{wc} between canard and tail. However, according to the experimental data for the modular model, only a change of vertical distance was needed to eliminate the negative effect of canard flow wake on the tail. When the horizontal distance between canard and tail is, $(h_{wc} + h_{wt}) = 6c$ or $7c$ the vertical distance between canard and tail must be $v_{wt} - v_{wc} = 2c$. If the horizontal distance was $(h_{wc} + h_{wt}) = 8c$ the vertical distance between canard and tail needed to eliminate canard effect on tail was $(v_{wt} - v_{wc}) = 2.5c$.

When the angle of attack was increased beyond the practical range, it was observed that the first flow separation occured on the canard, then the pitching moment slope gradient began to reduce and the neutral point was moved backwards.

The canard vertical position also affected zero lift pitching moment coefficient, C_{m_o}. The reason and effect was the same as in the case of canard-wing and conventional wing-tail configurations.

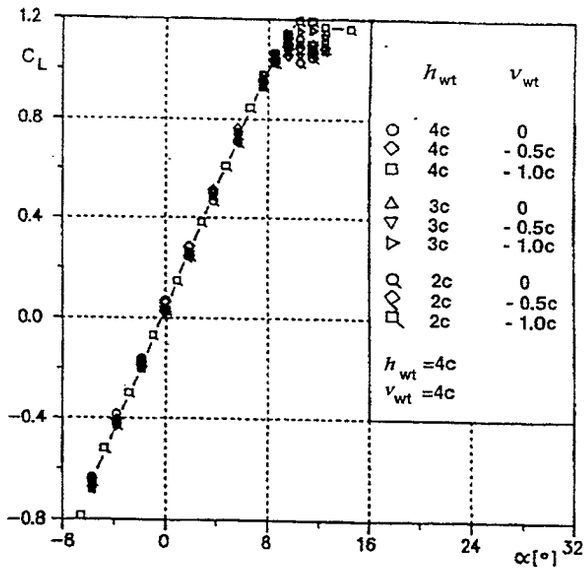

FIGURE 12 - Canard-Wing-Tail Configuration with HIgh Wing, Canard Effect

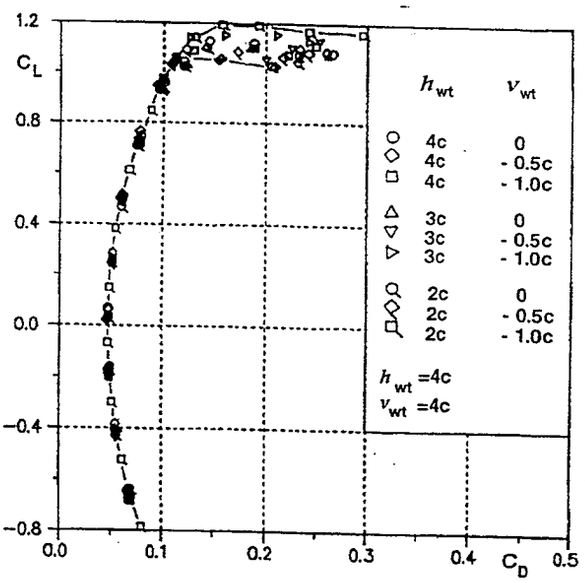

FIGURE 13 - Canard-Wing-Tail Configuration with HIgh Wing, Canard Effect

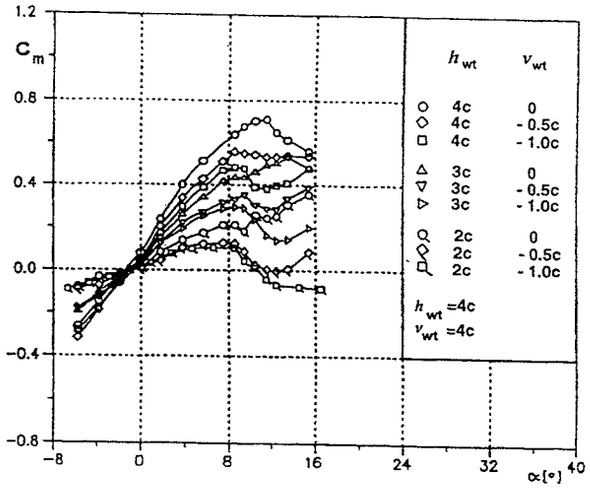

FIGURE 14 - Canard-Wing-Tail Configuration with HIgh Wing, Canard Effect

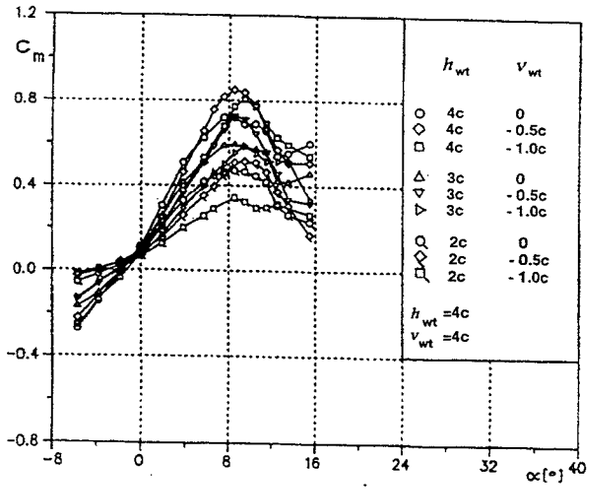

FIGURE 17 - Canard-Wing-Tail Configuration with LowWing, Canard Effect

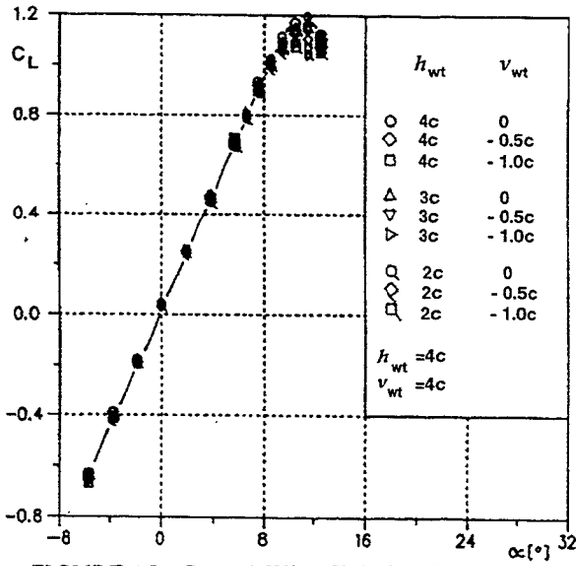

FIGURE 15 - Canard-Wing-Tail Configuration with Low Wing, Canard Effect

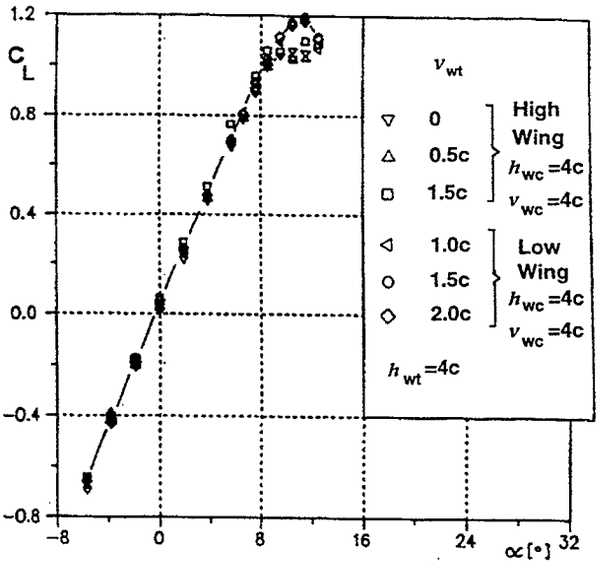

FIGURE 18 - Canard-Wing-Tail Configuration, Tail Effect

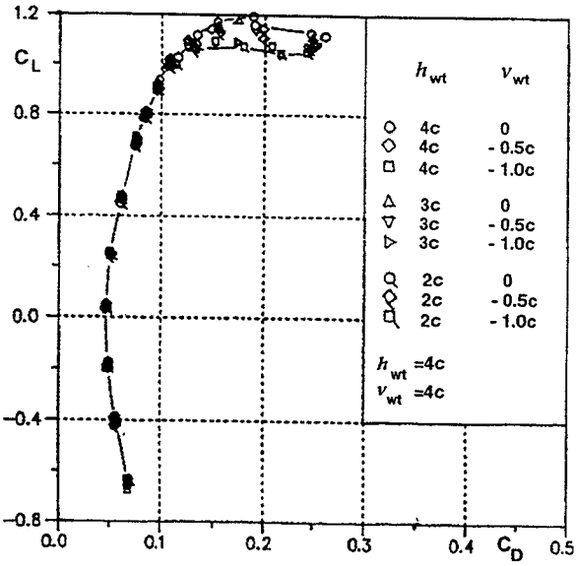

FIGURE 16 - Canard-Wing-Tail Configuration with Low Wing, Canard Effect

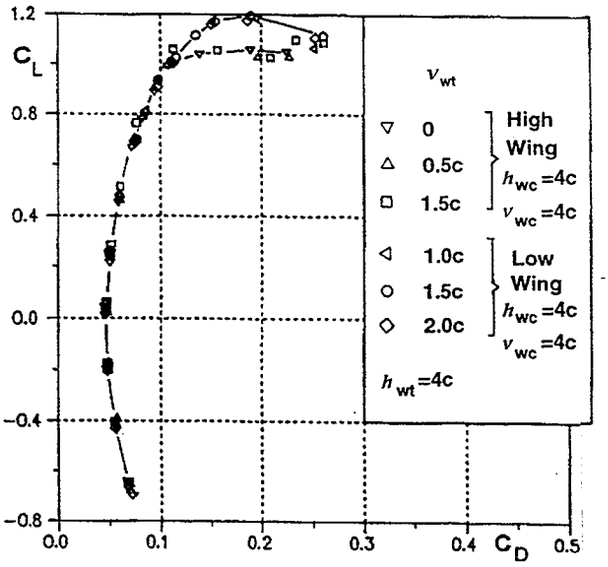

FIGURE 19 - Canard-Wing-Tail Configuration, Tail Effect

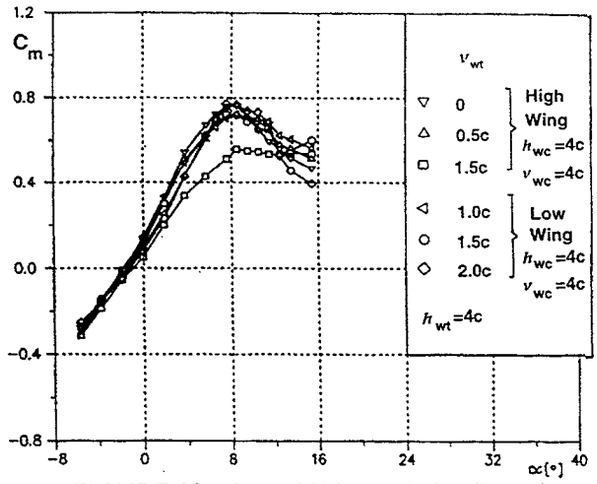

FIGURE 20 - Canard-Wing-Tail Configuration, Tail Effect

Numerical Modelling

To establish the effects of three aircraft geometrical layouts on aerodynamic characteristics, numerical calculations have been carried out for conventional, canard-wing and canard-wing-tail configurations. The numerical calculations were performed by using the commercial CFD package RAMPANT. This software was successfully used by the Department of Aerospace Engineering, University of Glasgow in 3-D numerical modelling in previous research work(8). The steps required for the numerical modelling process were as follows:

1. Defining the geometry with the DDN pre-processor.
2. Generating a 3-D unstructured boundary mesh on the defined geometry with the P-CUBE. The elements created in P-CUBE were Triangular-Surface. The boundary mesh of the aircraft in three surfaces configuration is shown in Figure 21.
3. Generating the 3-D unstructured volume mesh with the T-Grid software.
4. Importing the 3-D volume mesh into the solver RAMPANT 3-D. The first step of setting the problem in RAMPANT is to choose an adequate physical model. For this case the RNG $K-\varepsilon$ model was chosen which gives improved performance for separated flows and flows in curved geometry.

The Reynolds averaged Navier-Stokes equations were solved using a finite-volume approach. The integration method employed was an explicit multi-stage Runge-Kutta scheme.

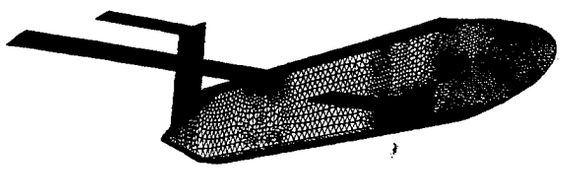

FIGURE 21 - The Boundary Mesh

Conclusions

The wind-tunnel tests and their results are presented for different canard-wing-tail aircraft configurations in low-speed applications. The data indicates that the interference between canard, wing and tail will affect basic aerodynamic characteristics with such intensity depending on relative position of all three lifting surfaces. A specially designed modular aircraft wind tunnel model was made. This model proved to be practical in creating a sufficient number of aircraft configurations. Obtained experimental data represents the aeronautical database for numerical validation which is currently performed in the Department of Aerospace Engineering at the University of Glasgow using the CFD code RAMPANT. Comparison of experimental and numerical data will be available in the future. Also, expirimental investigation into unconventional aircraft configuration will continue for balanced cases and different static margins.

Acknowledgements

This project has been supported by the VZLU, Aeronautical Research and Test Institute in Prague and the Department of Aerospace Engineering at the University of Glasgow. The authors acknowledges the help and support given by the leadership of both institutions.

References

(1) Keith, M.W., Selberg, B.P.. 'Aerodynamic Canard/Wing Parametric Analysis for General-Aviation Application', AIAA Journal of Aircraft, 1985.

(2) Selberg, B.P., Rokhsaz, K. 'Aerodynamic Tradeoff Study of Conventional Canard and Trisurface Aircraft Systems', AIAA Journal of Aircraft, 1986.

(3) Rokhsaz, K., Selberg, B.P. 'Analytical Study of Three-Surface Lifting Systems', Paper 850866, Society of Automotive Engineering Inc., 1986.

(4) Rokhsaz, K., Selberg, B.P. 'Three-Surface Aircraft: Optimum vs Typical', AIAA Journal of Aircraft, 1989.

(5) Feistel, T.W., Corsiglia, V.R., Levin, D.B., 'Wind-Tunnel Measurements of Wing-Canard Interference and a Comparison with Various Theories', Paper 810575, Society of Automotive Engineerings Inc., 1982

(6) Ostowar, C., Naik, D., 'An Experimental Study of a Three Lifting Surface Configuration', ICAS-86-1.94.

(7) Patek, Z. 'Basic Aerodynamic Characteristics of Some Unconventional Aircraft Configurations', CVUT Theses, 1991.

(8) Darida, M., Smrcek, L., Coton, F.N., 'Development of an RPV laboratory for In-Flight Aerofoil Testing', Paper, AIAA-97-2234.